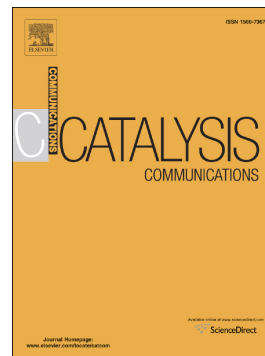


Accepted Manuscript

Palladium nanocatalysts in glycerol: Tuning the reactivity by effect of the stabilizer

Antonio Reina, Alejandro Serrano-Maldonado, Emmanuelle Teuma, Erika Martin, Montserrat Gómez



PII: S1566-7367(17)30415-6
DOI: doi:[10.1016/j.catcom.2017.10.004](https://doi.org/10.1016/j.catcom.2017.10.004)
Reference: CATCOM 5215
To appear in: *Catalysis Communications*
Received date: 20 July 2017
Revised date: 30 September 2017
Accepted date: 3 October 2017

Please cite this article as: Antonio Reina, Alejandro Serrano-Maldonado, Emmanuelle Teuma, Erika Martin, Montserrat Gómez, Palladium nanocatalysts in glycerol: Tuning the reactivity by effect of the stabilizer. The address for the corresponding author was captured as affiliation for all authors. Please check if appropriate. *Catcom*(2017), doi:[10.1016/j.catcom.2017.10.004](https://doi.org/10.1016/j.catcom.2017.10.004)

This is a PDF file of an unedited manuscript that has been accepted for publication. As a service to our customers we are providing this early version of the manuscript. The manuscript will undergo copyediting, typesetting, and review of the resulting proof before it is published in its final form. Please note that during the production process errors may be discovered which could affect the content, and all legal disclaimers that apply to the journal pertain.

Palladium nanocatalysts in glycerol: tuning the reactivity by effect of the stabilizer

Antonio Reina^a, Alejandro Serrano-Maldonado^b, Emmanuelle Teuma^a, Erika Martin^b, Montserrat Gómez^{a,*}

^a *Université de Toulouse, UPS, LHFA, 118 route de Narbonne, F-31062 Toulouse Cedex 9, France and CNRS, LHFA UMR 5069, F-31062 Toulouse Cedex 9, France. Fax: +33 561558204; Tel: +33 561557738; e-mail: gomez@chimie.ups-tlse.fr.*

^b *Departamento de Química Inorgánica, Facultad de Química, Universidad Nacional Autónoma de México, Av. Universidad 3000, 04510 México DF, México.*

Dedicated to the memory of Prof. Erika Martin (deceased, March 4th, 2017)

ABSTRACT: Palladium nanoparticles (PdNPs) prepared in neat glycerol containing TPPTS (tris(3-sulfophenyl)phosphine trisodium salt) or cinchona-based alkaloids (cinchonidine, quinidine) as capping agents, were applied as catalysts in fluoride-free Hiyama couplings and conjugate additions with the aim of evaluating the influence of the stabilizer in the catalytic reactivity. Therefore, PdNPs stabilized by phosphine favored C-C cross-couplings, whereas those containing alkaloids showed enhanced suitability for C-C homo-couplings and conjugate additions. The metal/stabilizer coordination mode, *i.e.* Pd-P dative bond and π - π interaction between quinoline moiety and palladium surface, is certainly key for the stabilization of different active metallic species and then promoting distinctive catalytic pathways.

Keywords: Palladium nanoparticles – Cinchona alkaloids – Phosphine – Glycerol – Hiyama couplings – Conjugate additions

1. Introduction

Palladium is one of the most used metals in catalysis, due to its versatility in inducing different types of activations (C-halide bonds by oxidative addition; C-H bonds by metalation; small molecules activation such as H₂ or CO...) [1]. This multipurpose reactivity finds its origin in the palladium ability for stabilizing different species exhibiting different oxidation states in the reaction medium: well-defined mono-metallic complexes, small clusters, nanoparticles, in addition to the distinctive reactivity of the extended metal surface [2,3]. The design of ligands and stabilizers together with the fine-tuning of the reaction conditions, enables the formation of a large variety of metal-based structures both at molecular and nanometric scale, involving dynamic equilibria among them [4]. This behavior can lead to a dual reactivity for palladium nanoparticles (PdNPs), both molecular- and surface-like, mainly when working under wet conditions, finding useful applications in one-pot multi-step processes (*e.g.* C-C coupling followed by hydrogenation) [5,6]. Furthermore, the nature of stabilizers can favor the formation of complexes or nanoclusters depending on their coordination ability [7]. Thus, polymers, which in general do not present strong interaction with metals, promote aggregated species (small clusters, nanoparticles) avoiding at the same time the formation of bulk metal. On the contrary, ligands involving strong Lewis donor centers (such as P- or S-based structures) can stabilize molecular complexes (both Pd(0) and Pd(II) species) using high ligand/metal ratios (at low ligand/metal ratios nanoparticles are also favored). Furthermore, ligands offering the possibility to interact with metal centers through aromatic moieties (π metal/ligand interaction), also lead to the stabilization of metal nanoparticles [8,9].

With the purpose of developing sustainable processes, the catalyst recovery (Pd/ligand or stabilizer systems) and in consequence its efficient immobilization, preserving both activity and selectivity, become crucial factors to obtain catalyst-free target organic products. The immobilization of PdNPs on solids has been extensively studied, involving a large variety of supports, *e.g.* carbon-based materials, zeolites, metal oxides, polymers or magnetic composites, among the most used [10,11].

However, PdNPs immobilized on liquid phases have been less considered, apart from the developed research with ionic liquids [12,13], including catalytic supported ionic liquid phases (SILP) [14-16] and functionalized membranes with poly(ionic liquids) [17,18]. Looking for alternative solvents showing suitable physico-chemical properties for synthesis and catalysis (*e.g.* high boiling point, negligible vapor pressure, high solubilizing ability for organic and inorganic compounds) [19-21], glycerol appeared as an appropriate choice taking into account that its H-bonded supramolecular structure [22], permits to confine metal nanoparticles. Glycerol enables an efficient immobilization of metal species, allowing at the same time a straightforward extraction of the corresponding organic products from the catalytic phase in the absence of metal [23,24]. In addition, its low vapor pressure permits direct analyses of the solution by TEM and XPS techniques [19-21]. Our previous work proved that PdNPs in glycerol containing two different types of stabilizers, TPPTS (tris(3-sulfophenyl)phosphine trisodium salt) and cinchona-based alkaloids (cinchonidine and quinidine), were efficient catalysts in molecular- (Suzuki, Heck and Sonogashira couplings) [23] and surface-like reactivity (hydrogenations and hydrodehalogenations) [24], respectively.

Herein, we have chosen the study of Hiyama coupling reactions with the aim of evaluating the differences in terms of selectivity towards homo- or cross-coupling pathways, induced by PdNPs of nearly the same size but capped by two different kinds of stabilizers, *i.e.* phosphine- and cinchona-based ligands. Furthermore, Michael conjugate additions permitted the coordination chemistry study at the palladium surface between stabilizers and reagents, revealing a positive catalytic effect in the case of PdNPs stabilized by quinidine.

2. Experimental

General details (materials and instrumental techniques), ligand exchange reactions at the palladium nanoparticles surface, ^{31}P NMR monitoring of the formation of palladium species during the oxidative addition step in Hiyama couplings, and characterization of both palladium nanoparticles and organic compounds obtained in the catalytic processes including their purification, are provided in the Supporting Information.

2.1. General procedure for the synthesis of palladium nanoparticles in glycerol, PdA-PdC

0.05 mmol of $\text{Pd}(\text{OAc})_2$ (11.2 mg) and 0.05 mmol of ligand (28.4 mg for TPPTS (A); 14.7 mg for cinchonidine (B); 16 mg for quinine (C)) were dissolved in 5 mL of glycerol and stirred under argon in a Fisher-Porter bottle at room temperature until complete dissolution. The system was then pressurized under 3 bar of dihydrogen and stirred at 80 °C for 18 h. A black colloidal solution was then obtained. Nanoparticles both in glycerol solution and at solid state were fully characterized by conventional techniques ((HR)TEM, IR, NMR, XPS, XRD, EA) [23,24].

2.2. General procedure for Pd-catalyzed Hiyama cross-coupling in glycerol

In a Schlenk tube, substrate (0.5 mmol), silane (0.6 mmol), base (1.5 mmol) and decane (71 mg, 0.5 mmol) as internal standard were added to 1 mL of preformed palladium nanoparticles (total amount of palladium 0.01 mmol) under argon. The reaction mixture was heated at 80 °C and stirred for the indicated time (3 – 24 h), and then cooled down to room temperature. The organic products were extracted from glycerol with dichloromethane (5 x 3 mL). The obtained products were previously described in the literature and their identification was carried out by comparison of their GC-MS data, ^1H and ^{13}C NMR spectra with the reported data (see Table S1 in the Supporting Information).

2.3. General procedure for Pd-catalyzed conjugate additions in glycerol

In a pressure cap tube, substrate (1 mmol), the corresponding amine, thiol or phosphine (1 mmol) and decane (71 mg, 1 mmol) as internal standard were added to 1 mL of preformed palladium nanoparticles (total amount of palladium 0.01 mmol) under argon. The reaction mixture was heated up to the desired temperature (35 – 100 °C) and stirred for the indicated time (0.25 – 24 h), and then cooled down to room temperature. Organic products were extracted from glycerol with dichloromethane (5 x 3 mL). The obtained products were previously described in the literature and their identification was done by comparison of their GC-MS data, ^1H and ^{13}C NMR spectra with the reported data (see Table S1 in the Supporting Information).

2.4. Catalytic phase recycling

For each kind of reaction (*i.e.* Hiyama reactions and conjugate additions), the catalytic phase recycling followed the same procedure. The first run was conducted as explained above (see 2.2 and 2.3 sections). After extraction of the organic products by a biphasic method using dichloromethane (5 x 3 mL), the glycerol phase was treated under vacuum at 50 °C for 1.5 h, and then cooled down to room temperature. Reagents were then added to the catalytic solution under argon as indicated above and the corresponding procedure was repeated.

3. Results and discussion

3.1. Synthesis and characterization of palladium nanocatalysts

In the present study, preformed PdNPs synthesized from $\text{Pd}(\text{OAc})_2$ in the presence of the corresponding stabilizer (A-C) in neat glycerol, under dihydrogen atmosphere, were used as catalysts, based on our previous studies (Scheme 1) [23,24]. The resulting black colloidal solutions were constituted by small (mean diameters in the range 1.4 – 2.1 nm), spherical and homogeneously dispersed Pd(0) nanoparticles as evidenced by TEM and XPS analyses (Figs. S1 and S2 in the

Supporting Information); PdNPs showed the same morphology in both colloidal solutions and solid state (Figs. S3 and S4 in the Supporting Information).

Scheme 1 HERE

3.2. Michael-type conjugate additions catalyzed by PdNPs stabilized by cinchona-based alkaloids

Substrates involved in aza-, thio- and phosphino-Michael conjugate additions present a remarkable coordination ability [25], which can trigger a displacement of the stabilizer present at the palladium surface. This coordination competition between substrate and stabilizer can serve as a rationale to explain the catalytic activity induced by the different catalytic systems. Thus, strong stabilizer coordination can lead to low catalytic activity; in contrast, labile stabilizers will be fast exchanged with the reagents favoring the corresponding conjugate addition. However, in this latter case, agglomeration issues can be observed due to the removal of the stabilizer from the surface, resulting in a loss of activity after the first run.

With the aim of studying the plausible lability of quinidine due to its weaker interaction with the palladium surface (by π interaction through the quinoline fragment) in comparison with TPPTS (by Pd-P dative bonds), we carried out a NMR monitoring study corresponding to the ligand exchange reaction between PdNPs stabilized by quinidine (**PdC** isolated at solid state by centrifugation from the glycerol phase) and TPPTS in a mixture of THF-*d*₈/D₂O (1/1), using triphenylphosphine oxide and cyclooctane as external standards (placed in a capillary in THF-*d*₈; see Fig. S5 in the Supporting Information). After 1 h, we observed the presence of free quinidine (as a mixture of quinidine and dihydroquinidine resulting of the partial hydrogenation of the vinyl group [24]) up to 60% in relation to the ligand present in the nanoparticles (0.01 mmol) and simultaneously, the signal disappearance of free TPPTS caused by its approach to the palladium surface, up to 62% in relation to the added phosphine (for details, see Experimental part in the Supporting Information); this means that *ca.* 60% of the cinchona ligand was replaced by the added phosphine. However, when the ligand exchange was done starting with palladium nanoparticles stabilized by phosphine, *i.e.* **PdA**, in the presence of free quinidine, no exchange was observed, corroborating the robustness of the TPPTS bonded at the palladium surface.

With the purpose of evidencing this effect by catalytic reactivity, we tested **PdA**, **PdB** and **PdC** as catalytic precursors in the chosen benchmark base-free reaction between acrylonitrile (**1**) and morpholine (**a**) (Table 1). No important differences were observed under harsh conditions (100 °C, 1 mol% Pd), giving more than 93% yield towards the desired product **1a** (entries 1-3, Table 1); the catalytic phases remained as black colloidal solutions. However, the catalytic system **PdC** (stabilized by quinidine) was also highly active under smoother conditions, leading to 80% yield using 0.1 mol% palladium load at 80 °C in 2 h (entry 4, Table 1); under these conditions, **PdA**, stabilized by TPPTS, only afforded 50% conversion after 12 h of reaction (entry 5, Table 1). The reaction was monitored during the first hour by GC-MS, evidencing that the catalyst remains active during the process and showing a TOF of 1,440 h⁻¹ after 15 min of reaction; the initial reaction rates (calculated between 6 and 12 min, meaning up to 25% conversion) were in the range 2.5x10⁻³ – 3.5x10⁻³ molL⁻¹s⁻¹ (see Fig. S6 in the Supporting Information). Accordingly, **PdC** was efficiently recycled up to ten times without significant activity loss (Fig. 1); ICP analyses indicated a negligible loss of palladium after each run (0.004 – 0.01 ppm, determined by ICP-OES) and the absence of quinidine. To the best of our knowledge, **PdC** represents the most efficient and recyclable catalyst for Michael-type additions reported up to now [23,26].

Table 1 HERE

Figure 1 HERE

The reaction scope involving primary (**b,c**) and secondary (**d**) amines, aqueous ammonia (**e**), thiols (**f, g**) and secondary phosphines (**h, i**) is illustrated in Scheme 2, using **PdC** as catalytic precursor. In all cases, the reaction proceeded selectively, leading to the expected products in high yields, except for the alkyl thiol (**g**) and secondary phosphine (**i**) where moderate conversions (31-67%) and yields (26-64%) were obtained. No asymmetric induction was prompted using methacrylonitrile (**3**) as prochiral substrate using morpholine, cyclohexylamine and 4-methylthiophenol as Michael donor reagents (see Table S2 and Fig. S7 in the Supporting Information). This result is in agreement with the de-coordination of the cinchona-based stabilizer from the palladium surface that permits the conjugate addition.

To sum up, the high activity shown by **PdC** compared with **PdA** agrees with the higher coordination lability of the cinchona-based stabilizers than that exhibited by TPPTS. Quinidine can be de-coordinated from the metal surface in the presence of donor compounds (such as N-, S- or P-based reagents), favoring then the coordination of reagents at the palladium surface followed by the conjugate addition, which can be otherwise obstructed in the presence of the bulky phosphine TPPTS. The efficient recycling of the catalytic phase together with the absence of quinidine in the products seem to indicate that the cinchona stabilizer coordinates again at the palladium surface after the reaction is completed. Moreover, this catalytic behavior showed the positive role of palladium nanoparticles in conjugate additions (for control tests, see Table S3 in the Supporting Information).

Scheme 2 HERE

3.3. Hiyama cross-couplings catalyzed by PdNPs in glycerol

It is very well-known that Pd-catalyzed C-C cross-couplings promoted by nanoparticles in wet phases, work under homogeneous regime, *i.e.* preformed nanoparticles act as reservoirs of catalytically active molecular species in particular for Heck reactions [5,27]. However, C-C homo-couplings can involve activations of reagents at the metal surfaces through single electron transfer paths [28,29]. Taking into account the different surface state caused by TPPTS and alkaloids **B** and **C**, we envisaged that phosphines and alkaloids could favor different mechanisms for C-C couplings and therefore give different products (*i.e.* homo-coupling or cross-coupling compounds) starting from the same reagents. For this study, we chose the Hiyama C-C cross-coupling reaction because it represents a more attractive way for the synthesis of biphenyls than other cross-couplings, such as Stille (involving organotin reagents) or Suzuki (involving organoboron derivatives) reactions, due to the intrinsic properties of organosilanes, such as stability, easy handling and low toxicity, together with the straightforward conversion of the silicon-based by-products in innocuous silica waste [30].

Due to the scarce works reported in the literature using preformed PdNPs as catalytic precursors [30,31], we first optimized the reaction conditions using **PdA** in glycerol for the catalytic reactions of bromo-arenes [4-bromobenzotrifluoride (**4Br**), 4-bromonitrobenzene (**5Br**) and 4-bromobenzonitrile (**6Br**)] and trimethoxyphenylsilane (**j**) as reagents (Table S4 in the Supporting Information). Under these conditions, we studied the coupling between substrates containing both electron-withdrawing (**4-7**) and electro-donor groups (**8-10**) (Table 2). For substrates exhibiting electron-withdrawing groups in *para*-position (**4-6**), full conversions and excellent selectivity towards the corresponding cross-coupling products (**CC**) were obtained for 4-bromobenzotrifluoride (**4Br**) and 4-bromobenzonitrile (**6Br**) (entries 1 and 3, Table 2). At shorter times (3 h), the selectivity was preserved (entry 4, Table 2). Special mention should be made in the case of 4-bromonitrobenzene (**5Br**), which reached almost complete conversion in a short time (3 h), leading to a nearly equimolar mixture of **5j** and **5HC**, and in consequence evidencing a strong competition between the transmetalation step (to give **5j**) and the homocoupling reaction (to give **5HC**) (entry 2, Table 2). The monitoring of this reaction at 3 h and 24 h using a low catalyst load (1 mol%), indicated that the cross-coupling reaction is faster at high concentrations of silylated reagent, but after *ca.* 50% conversion, the transmetalation step seems to slow down, favoring the formation of the corresponding **HC** product (see entries 6-7, Table S4 in the

Supplementary Material). In the case of 2-bromobenzonitrile (**7Br**), the steric hindrance of the CN group undoubtedly prevents the oxidative addition of the arylbromide to the metal center and as a result the reaction did not proceed (entry 5, Table 2). As expected, for substrates containing electron-donor groups (entries 6-8, Table 2), yields were lower than those obtained with activated arylbromides (entries 1-4, Table 2), and the selectivity towards the **HC** product was higher in particular for 4-bromotoluene (entry 8, Table 2) where **10HC** was mainly obtained. However, for 4-bromoanisole (**8Br**), the **CC** product was privileged (entry 6, Table 2), probably due to the interaction of the methoxide group with the palladium surface, thus favoring the oxidative addition step [33]. Chloroarenes **4Cl** and **6Cl** (entries 9-10, Table 2), despite containing electron-withdrawing substituents, only gave low-to-moderate conversions. The hard activation of the C-Cl bond may lead to a different mechanism than the conventional Hiyama cross-coupling pathway, mainly producing the homocoupling product [34,35]. Analogously to trimethoxy(phenyl)silane (**j**), **PdA** catalyzed the coupling between vinyltrimethylsiloxane (**k**) and 4-bromobenzotrifluoride (**4Br**) and 4-bromobenzonitrile (**6Br**), showing a high activity and selectivity towards the **CC** product (> 90% conversion after 3 h of reaction; see Scheme S1 in the Supporting Information); only small amounts of oligomers were detected by GC (< 8%).

Table 2 HERE

It is important to highlight that for the reactions mainly giving the homocoupling product (**HC**), the reaction medium remained as a black colloidal solution after catalysis, suggesting that the formation of **HC** products arises from the surface reactivity of the palladium nanoparticles. In contrast, for the reactions where the cross-coupling product (**CC**) was predominant, orange solutions were observed once the process started, certainly due to the palladium leaching from the starting nanoparticles to give molecular active complexes, specially favored by TPPTS.

These results indicate that for the substrates triggering a fast halo-arene oxidative addition, the formation of homogeneous Pd(II) molecular species is preferred and then the cross-coupling process takes place under a homogeneous regime. On the contrary, when the formation of Pd(II) species is impeded (slow oxidative addition), in spite of the presence of phosphine, single electron transfer paths are privileged [29], promoting a surface reactivity towards the homocoupling product. Actually, the behavior of palladium in the presence of TPPTS was monitored by ³¹P NMR. Palladium acetate and TPPTS in glycerol at 80 °C gave an orange solution, showing the apparition of a new signal at *ca.* 30 ppm (see Fig. S8 and Experimental section in the Supporting Information), evidencing the formation of a Pd(II) complex, which decomposes in the presence of H₂, giving a black colloidal solution of PdNPs (with absence of NMR signals). Further addition of a bromo-arene, such as 4-bromobenzotrifluoride, triggered the formation of Pd(II) complexes by oxidative addition on Pd(0), observing again signals in the region 20-30 ppm; the resulting orange solution was stable at 80 °C for long time (up to 24 h).

In the case of PdNPs stabilized by alkaloids (**PdB** and **PdC**) under the previously optimized conditions, the Hiyama couplings only gave the corresponding homocoupling products (Table 3). Curiously, **PdB** was more active than **PdC** (entries 2, 5 and 8 vs 3, 6 and 9, Table 3), probably due to the stronger interaction of **C** with the palladium surface than that with **B**, due to the presence of the methoxide group on the quinoline fragment [8,9,33]. This lack of reactivity of **PdB** and **PdC** to give the expected Hiyama C-C cross-coupling products contrary to the efficiency exhibited by **PdA**, correlates with the inactivity observed of **PdB** and **PdC** in other C-C cross-couplings using aryl bromides as substrates (see Tables S5-S7 in the Supporting Information for Heck, Suzuki and Sonogashira reactions, respectively).

Table 3 HERE

This change on the reactivity (**PdA** vs **PdB** or **PdC**, Scheme 3) can be associated to both the different type of interaction of stabilizers with the metallic surface and the oxidative addition step rate. It is known that cinchona ligands privilege the π aromatic coordination through the quinoline fragment [8,9,24], probably due to the weak N-Pd bond in contrast to the stronger P-Pd bond, because of the π -back donation of Pd to phosphorus. Thus, metal leaching and further stabilization of Pd(II) molecular complexes are favored with phosphine-type ligands. In consequence, the cross-coupling path is inhibited for PdNPs containing cinchonas, which usually operates under homogeneous regime conditions. However, homocoupling processes are commonly favored at the surface of palladium nanoparticles as previously described in the literature [28,29,34,35]. In the absence of any ligand as stabilizer (*i.e.* no dative interactions between ligand and nanoparticle), PdNPs only favor the formation of cross-coupling products (see Table S8 in the Supporting Information for related reported works).

Scheme 3 HERE

In conclusion, with this study, we proved how the capping agent permits to tune the catalytic reactivity (for both Michael conjugate additions and Hiyama couplings), using the same type of PdNPs in terms of size, morphology, and surface state, when the nature of the stabilizer is changed. The catalytic results obtained in this paper not only prove the efficiency of PdNPs in different C-C and C-heteroatom bond formation processes, but also offer a useful approach to rationalize the reaction pathways using palladium nanoparticles as catalytic precursors.

Acknowledgements

Financial support from the Centre National de la Recherche Scientifique (CNRS), the Université de Toulouse 3- Paul Sabatier, the Associated International Laboratory LIA-LCMMC and CONACYT FOINS-246968 are gratefully acknowledged. A.R. and A.S.-M. thank CONACYT for PhD grants.

Supplementary data

Supplementary data to this article can be found online at <http://>

References

- [1] For a selected contribution, see: J. Tsuji, *Palladium reagents and catalysts*, John Wiley & Sons, Sussex, 2004.
- [2] B. M. Trost, *Tetrahedron* 71 (2015) 5708-5733.
- [3] I. Favier, D. Madec, E. Teuma, M. Gómez, *Curr. Org. Chem.* 15 (2011) 3127-3174.
- [4] For a selected contribution, see: R. Ciriminna, V. Pandarus, A. Fidalgo, L.M. Ilharco, F. Béland, M. Pagliaro, *Org. Process Res. Dev.* 19 (2015) 755-768.
- [5] S. Jansat, J. Durand, I. Favier, F. Malbosc, C. Pradel, E. Teuma, M. Gómez, *ChemCatChem* 1 (2009) 244-246.
- [6] A. M. López-Vinasco, I. Guerrero-Ríos, I. Favier, C. Pradel, E. Teuma, M. Gómez, E. Martin, *Catal. Commun.* 63 (2015) 56-61.
- [7] For a critical review concerning the role of different types of capping agents in the stabilization of metal nanoparticles, see L. Starkey Ott, R.G. Finke, *Coord. Chem. Rev.* 251 (2007) 1075-1100.
- [8] I. Favier, S. Massou, E. Teuma, K. Philippot, B. Chaudret, M. Gómez, *Chem. Commun.* (2008) 3296-3298.
- [9] A. Vargas, A. Baiker, *J. Catal.* 239 (2006) 220-226.
- [10] M.J. Climent, A. Corma, S. Iborra, M.J. Sabater, *ACS Catal.* 4 (2014) 870-891.
- [11] M.B. Gawande, P.S. Branco, R.S. Varma, *Chem. Soc. Rev.* 42 (2013) 3371-3393.
- [12] I. Favier, D. Madec, M. Gómez, in Chapter 5 "Metallic nanoparticles in ionic liquids. Applications in catalysis" in "Nanomaterials in catalysis", Eds. K. Philippot and P. Serp, Wiley-VCH, Weinheim, 2013, pp 203-249.
- [13] M.H.G. Pechtl, J.D. Scholten, J. Dupont, *Molecules* 15 (2010) 3441-3461.
- [14] L. Luza, C.P. Rambor, A. Gual, F. Bernardi, J.B. Domingos, T. Grehl, P. Bruner, J. Dupont, *ACS Catal.* 6 (2016) 6478-6486.
- [15] H.-P. Steinruck, J. Libuda, P. Wasserscheid, T. Cremer, C. Kolbeck, M. Laurin, F. Maier, M. Sobota, P. S. Schulz, M. Stark, *Adv. Mater.* 23 (2011) 2571-2587.
- [16] L. Rodriguez-Perez, C. Pradel, P. Serp, M. Gómez, E. Teuma, *ChemCatChem* 3 (2011) 749-754.
- [17] Y. Gu, I. Favier, C. Pradel, D.L. Gin, J.-F. Lahitte, R.D. Noble, M. Gómez, J.-C. Remigy, *J. Membrane Sci.* 492 (2015) 331-339.
- [18] V.W. Faria, D.G.M. Oliveira, M.H.S. Kurz, F.F. Gonçalves, C.W. Scheeren, G.R. Rosa, *RSC Adv.* 4 (2014) 13446-13452.
- [19] F. Chahdoura, I. Favier, M. Gómez, *Chem. Eur. J.* 20 (2014) 10884-10893.
- [20] Y. Gu, F. Jérôme, *Green Chem.* 12 (2010) 1127-1138.
- [21] A. E. Díaz-Alvarez, J. Francos, B. Lastra-Barreira, P. Crochet, V. Cadierno, *Chem. Commun.* 47 (2011) 6208-6227.
- [22] T. Kusakawa, G. Niwa, T. Sasaki, R. Oosawa, W. Himeno, M. Kato, *Bull. Chem. Soc. Jpn.* 86 (2013) 351-353.

- [23] F. Chahdoura, C. Pradel, M. Gómez, *Adv. Synth. Catal.* 355 (2013) 3648-3660.
- [24] A. Reina, C. Pradel, E. Martin, E. Teuma, M. Gómez, *RSC Adv.* 6 (2016) 93205-93216.
- [25] For a selected review, see: A. Gutnov, *Eur. J. Org. Chem.* (2008) 4547-4554 and references therein.
- [26] For a selected contribution involving PdNPs, see: M. Saha, A. K. Pal, *Adv. Nanoparticles*, 1 (2012) 61-70.
- [27] N.T.S. Phan, M. Van der Sluys, C. W. Jones, *Adv. Synth. Catal.* 348 (2006) 609-679.
- [28] S. Mukhopadhyay, G. Rothenberg, D. Gitis, H. Wiener, Y. Sasson, *J. Chem. Soc., Perkin Trans. 2* (1999) 2481-2484.
- [29] M. Zeng, Y. Du, L. Shao, C. Qi, X.-M. Zhang, *J. Org. Chem.* 75 (2010) 2556-2563.
- [30] H.F. Sore, W.R.J.D. Galloway, D.R. Spring, *Chem. Soc. Rev.* 41 (2012) 1845-1866.
- [31] B.C. Ranu, R. Dey, K. Chattopadhyay, *Tetrahedron Lett.* 49 (2008) 3430-3432.
- [32] D. Srimani, A. Bej, A. Sarkar, *J. Org. Chem.* 75 (2010) 4296-4299.
- [33] D. Sanhes, D. Raluy, S. Rétory, N. Saffon, E. Teuma, M. Gómez, *Dalton Trans.* 39 (2010) 9719-9726.
- [34] S. Xu, H. Sheng, S. Liao, D. Hu, D. Yu, T. Ye, *Catal. Commun.* 89 (2017) 121-124.
- [35] X. Li, D. Li, Y. Bai, C. Zhang, H. Chang, W. Gao, W. Wei, *Tetrahedron* 72 (2016) 6996-7002.

CAPTIONS FOR FIGURES, SCHEMES AND TABLES

Scheme 1. Synthesis of PdNPs containing TPPTS (**PdA**) and cinchona-based ligands, cinchonidine (**PdB**) and quinidine (**PdC**).

Scheme 2. Compounds obtained by Pd-catalyzed conjugate additions from acceptor substrates (**1**, **2**) using different Michael donor reactants (**a-i**). Figures correspond to conversions (yields). Reaction conditions: 1 mol% **PdC**, 100 °C, 2 h (or 24 h); conversions and yields determined by GC using decane as internal standard.

Scheme 3. Schematic representation of the pathways for Hiyama couplings catalyzed by PdNPs based on the nature of the stabilizer.

Fig. 1. Palladium-catalyzed C-N bond formation by direct reaction of acrylonitrile (**1**) and morpholine (**a**). Diagram showing the recycling of the catalytic phase. Figures indicate yield of **1a** after each recycling (see entry 3 of Table 1 for reaction conditions).

Table 1. Pd-catalyzed C-N bond formation between acrylonitrile and morpholine by Michael-type addition.

Table 2. Pd-catalyzed Hiyama cross-coupling reactions with aryl halides.

Table 3. Effect of the nature of stabilizers under Pd-catalyzed Hiyama cross-coupling conditions.

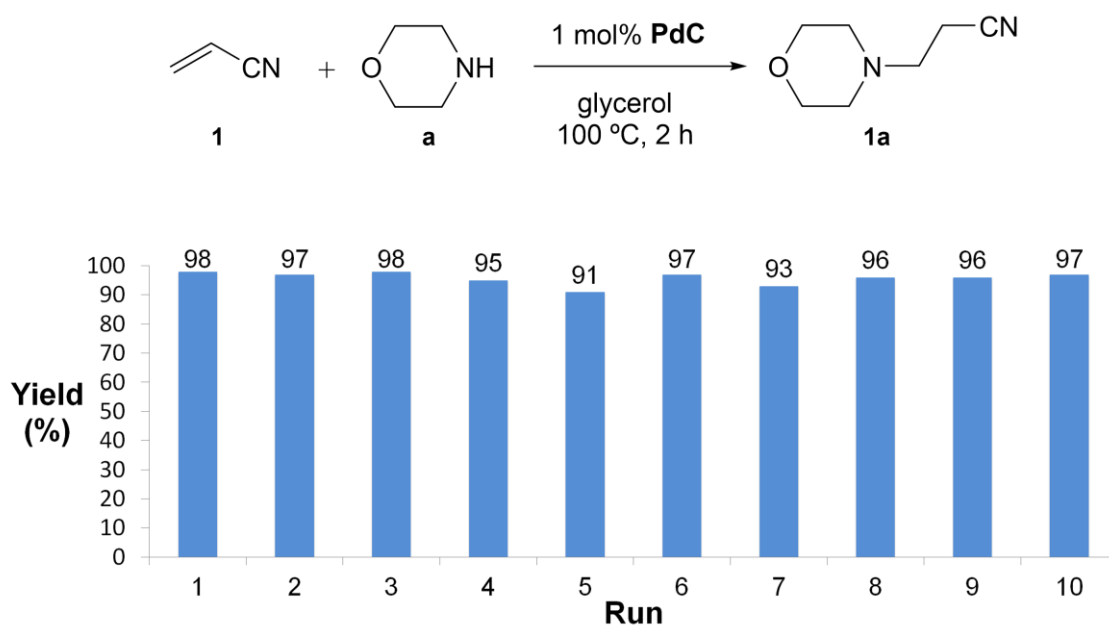
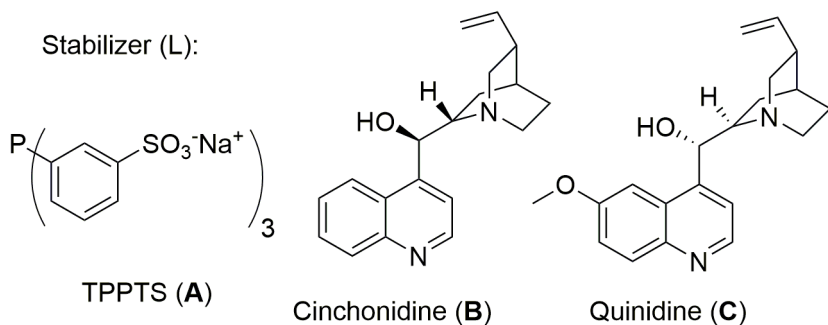
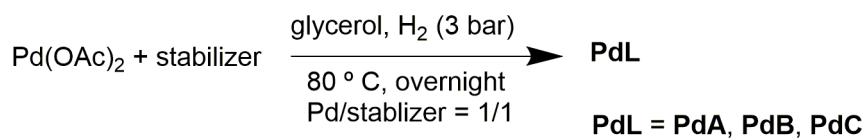
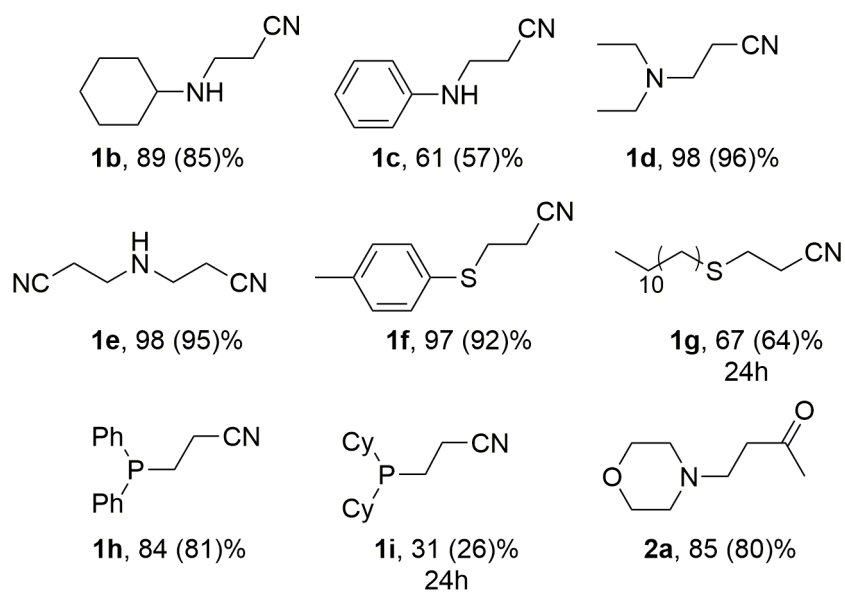


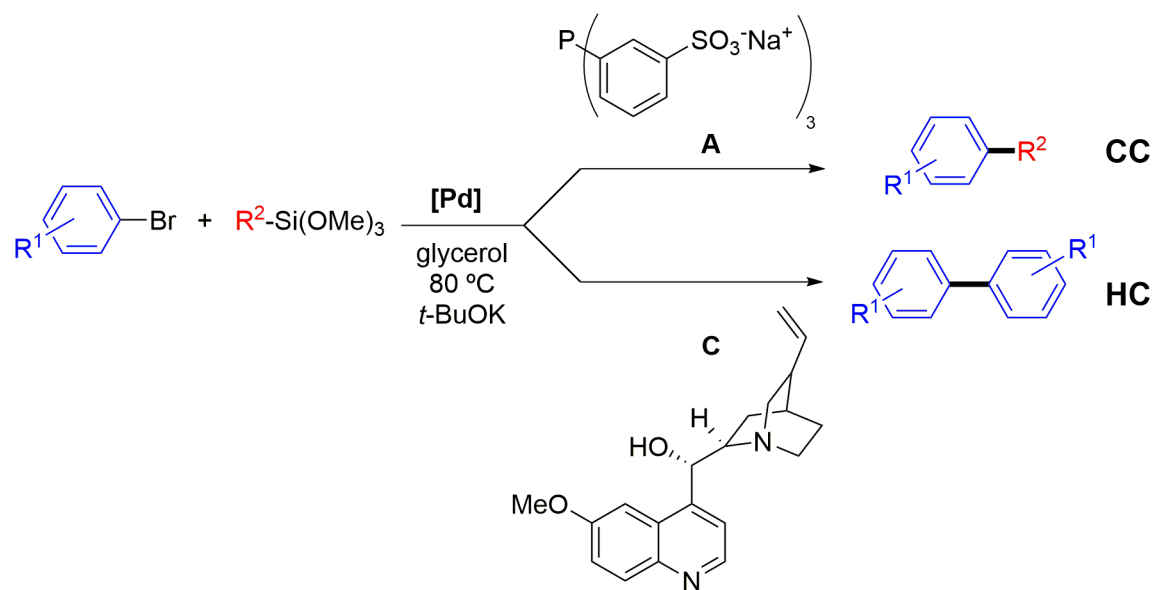
Figure 1



Scheme 1



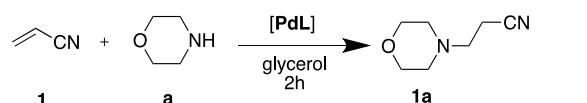
Scheme 2



Scheme 3

Table 1

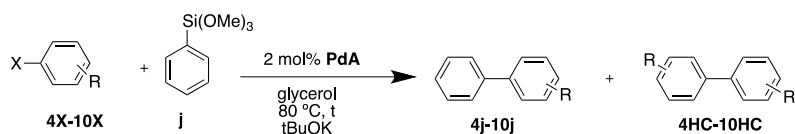
Pd-catalyzed C-N bond formation between acrylonitrile and morpholine by Michael-type addition.^a



The reaction scheme shows acrylonitrile (1) reacting with morpholine (a) in the presence of a palladium catalyst [PdL] in glycerol for 2 hours to produce N-(2-cyanoethyl)morpholine (1a).

Entry	Catalyst (load, mol%)	T (°C)	Conv. (yield) ^b (%)
1 ^c	PdA (1)	100	>99 (98)
2	PdB (1)	100	98 (93)
3	PdC (1)	100	>99 (98)
4	PdC (0.1)	80	85 (80)
5 ^c	PdA (0.1)	80	50 (44)

^a Results from duplicated experiments. Reaction conditions: 1 mmol of acrylonitrile (**1**), 1 mmol of morpholine (**a**) and 1 mL of the catalytic glycerol solution of **PdA**, **PdB** or **PdC** (10^{-2} molL⁻¹, 0.01 mmol of total Pd) for 2 h. ^b Determined by GC using decane as internal standard. ^c See reference [23].

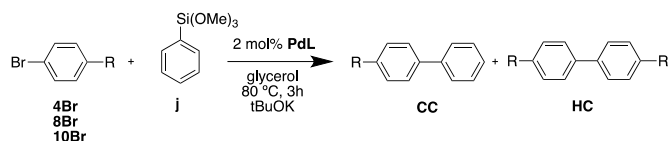
Table 2.Pd-catalyzed Hiyama cross-coupling reactions with aryl halides.^a

Entry	Substrate	R	t (h)	Conv(%) ^b	Selectivity CC/HC (%) ^{b,c}
1	4Br	4-CF ₃	24	>99	90/10 (4j/4HC)
2	5Br	4-NO ₂	3	91	57/43 (5j/5HC)
3	6Br	4-CN	24	>99	95/5 (6j/6HC)
4	6Br	4-CN	3	42	100/0 (6j)
5	7Br	2-CN	24	<5	-
6	8Br	4-OCH ₃	24	75	92/8 (8j/8HC)
7	9Br	4-SCH ₃	24	78	72/28 (9j/9HC)
8	10Br	4-CH ₃	24	86	11/89 (10j/10HC)
9	4Cl	4-CF ₃	24	36	20/80 (4j/4HC)
10	6Cl	4-CN	24	75	0/100 (6HC)

^a Results from duplicated experiments. Reaction conditions: 0.5 mmol of aryl halide (**4-10**), 0.6 mmol of trimethoxy(phenyl)silane (**j**), 1.5 mmol of *t*BuOK and 1 mL of the catalytic glycerol solution of **PdA** ($10^{-2} \text{ molL}^{-1}$, 0.01 mmol of total Pd). ^b Conversion and selectivity determined by GC using decane as internal standard. ^c In brackets, labels corresponding to the products formed; **CC** denotes cross-coupling product; **HC** denotes homocoupling product.

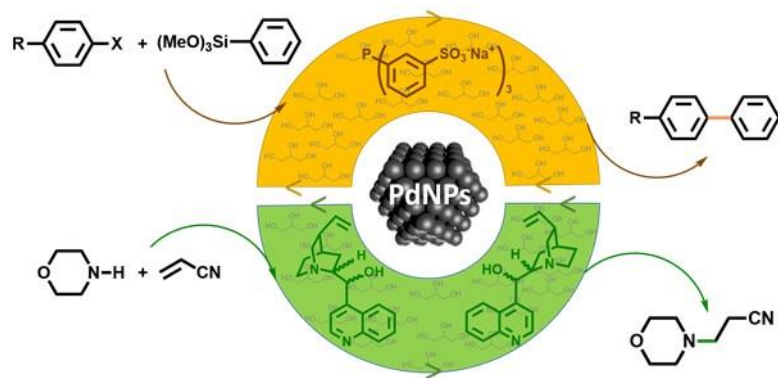
Table 3.

Effect of the nature of stabilizers under Pd-catalyzed Hiyama cross-coupling conditions.^a



Entry	PdL	Substrate	R	Conv. (%) ^a	Selectivity CC/HC (%) ^{b,c}
1	PdA	4Br	CF ₃	>99	90/10 (3j/3HC)
2	PdB	4Br	CF ₃	92	0/100 (3HC)
3	PdC	4Br	CF ₃	26	0/100 (3HC)
4	PdA	8Br	OCH ₃	75	92/8 (7j/7HC)
5	PdB	8Br	OCH ₃	24	0/100 (7HC)
6	PdC	8Br	OCH ₃	9	n.d. ^d
7	PdA	10Br	CH ₃	86	11/89 (9j/9HC)
8	PdB	10Br	CH ₃	24	0/100 (9HC)
9	PdC	10Br	CH ₃	10	n.d. ^d

^a Results from duplicated experiments. Reaction conditions: 0.5 mmol of aryl halide, 0.6 mmol of trimethoxy(phenyl)silane (**j**), 1.5 mmol of *t*BuOK and 1 mL of the catalytic glycerol solution of **PdA**, **PdB** or **PdC** (10⁻² molL⁻¹, 0.01 mmol of total Pd). ^b Conversion and selectivity determined by GC using decane as internal standard. ^c In brackets, labels corresponding to the products formed; **CC** denotes cross-coupling product; **HC** denotes homocoupling product. ^d Only homocoupling was detected.



Graphical abstract

ACCEPTED MANUSCRIPT

HIGHLIGHTS

- Palladium nanoparticles dispersed in glycerol led to versatile catalysts
- Stabilizer coordination mode at the metal surface tunes the catalytic reactivity
- The TPPTS phosphine privileged C-C cross-couplings
- Cinchona-based stabilizers induced surface-like reactivity
- Catalytic glycerol phase was efficiently recycled

ACCEPTED MANUSCRIPT